AIAA JOURNAL
Vol. 40, No. 3, March 2002

Asymptotic Theory for Laminated Piezoelectric Circular Cylindrical Shells

Zhen-Qiang Cheng* and J. N. Reddy†
Texas A&M University, College Station, Texas 77843-3123

An asymptotic theory is presented for laminated piezoelectric circular cylindrical shells under electromechanical loads. The three-dimensional coupled electromechanical problem reduces to a hierarchy of two-dimensional equations, which can be solved systematically. The proposed theory is illustrated by considering two example problems. Numerical results show excellent agreement with an available exact solution and also provide some suggestions in establishing new two-dimensional piezoelectric shell models.

I. Introduction

RECENT rigorous studies[1–9] have revealed some deficiencies in many existing two-dimensional piezoelectric plate models. For example, the deflection distribution is not nearly constant through the thickness of a thick plate under thermal and/or electric loads. The in-plane electric field components are not negligible in the case of unequal normal electric displacements on the top and bottom surfaces of a plate. In contrast, the in-plane electric field components may be larger in magnitude than the transverse electric field component in this case. The electric potential is piecewisely smoothly (or zigzag) distributed through the thickness of a laminated piezoelectric plate. Accordingly, more efficient and reliable theories to improve these assumptions have been desirable for analyzing the electromechanical and thermomechanical problems.

In recent developments, asymptotic theories have been proposed for elastic plates,[10–15] piezoelectric plates,[5–9,16,17] and circular cylindrical elastic shells.[18] An important result is that solutions of the three-dimensional equations may be generated by solving two-dimensional equations hierarchically. There is no need for making any assumptions a priori. The present paper intends to establish an asymptotic theory for laminated circular cylindrical piezoelectric shells.

II. State-Space Equations

The linear constitutive equations of a piezoelectric medium are[19]

$$\boldsymbol{\tau} = \boldsymbol{c} : \boldsymbol{S} - \boldsymbol{e}^T \cdot \boldsymbol{E}, \qquad \boldsymbol{D} = \boldsymbol{e} : \boldsymbol{S} + \boldsymbol{k} \cdot \boldsymbol{E} \tag{1}$$

where $\boldsymbol{\tau}$ and $\boldsymbol{S}$ are the symmetric stress and strain tensors; $\boldsymbol{D}$ and $\boldsymbol{E}$ the electric displacement and the electric field vectors; and $\boldsymbol{c}$, $\boldsymbol{e}$, and $\boldsymbol{k}$ the elastic, piezoelectric, and dielectric moduli.

The equations of equilibrium and the charge equation in the absence of body forces and electric charge density are given in the cylindrical coordinate system $\{r, \theta, x\}$ as

$$\begin{gathered} r^{-1}(r\tau_{rr})_{,r} + r^{-1}\tau_{r\theta,\theta} - r^{-1}\tau_{\theta\theta} + \tau_{rx,x} = 0 \\ r^{-2}\left(r^2\tau_{r\theta}\right)_{,r} + r^{-1}\tau_{\theta\theta,\theta} + \tau_{\theta x,x} = 0 \\ r^{-1}(r\tau_{rx})_{,r} + r^{-1}\tau_{\theta x,\theta} + \tau_{xx,x} = 0 \\ r^{-1}(rD_r)_{,r} + r^{-1}D_{\theta,\theta} + D_{x,x} = 0 \end{gathered} \tag{2}$$

The strain-displacement relations and the electric field-potential relations are

$$\begin{gathered} S_{rr} = u_{r,r}, \qquad S_{\theta\theta} = r^{-1}u_{\theta,\theta} + r^{-1}u_r, \qquad S_{xx} = u_{x,x} \\ 2S_{rx} = u_{x,r} + u_{r,x}, \qquad 2S_{r\theta} = r^{-1}u_{r,\theta} + r\left(r^{-1}u_\theta\right)_{,r} \\ 2S_{\theta x} = u_{\theta,x} + r^{-1}u_{x,\theta}, \qquad E_r = -\varphi_{,r} \\ E_\theta = -r^{-1}\varphi_{,\theta}, \qquad E_x = -\varphi_{,x} \end{gathered} \tag{3}$$

Consider a circular cylindrical piezoelectric panel of uniform thickness h and inner radius r_0, as shown in Fig. 1. The inner surface of the panel is designated to be the reference surface. Let the circumferential, axial, and normal length parameters be $x_1 = r_0\theta$, $x_2 = x$, and $x_3 = r - r_0$, respectively.

Hereafter, a comma followed by a subscript i denotes the partial derivative with respect to x_i, and a repeated index, unless specified otherwise, implies summation over the range of the index with Latin indices ranging from 1 to 3 and Greek indices from 1 to 2.

For monoclinic piezoelectric materials with reflectional symmetry in surfaces parallel to the surfaces of the circular cylindrical shell, the following state-space equation may be formulated from Eqs. (1–3):

$$\begin{bmatrix} \boldsymbol{Q}_F^{-1}\boldsymbol{F} \\ \boldsymbol{Q}_G^{-1}\boldsymbol{G} \end{bmatrix} = \varepsilon \begin{bmatrix} \varepsilon\boldsymbol{P} & \boldsymbol{A} \\ \boldsymbol{B} & -\varepsilon\boldsymbol{P}^T \end{bmatrix} \begin{bmatrix} \boldsymbol{F} \\ \boldsymbol{G} \end{bmatrix} + \varepsilon^3\eta \begin{bmatrix} \tilde{\boldsymbol{A}}\,\boldsymbol{G} \\ \boldsymbol{0} \end{bmatrix} \tag{4}$$

$$\begin{gathered} \tau_{\alpha\beta} = \left(r_0 r^{-1} L_{\beta 1}^{\alpha\omega}\partial_1 + L_{\beta 2}^{\alpha\omega}\partial_2\right)u_\omega + r^{-1}L_{\beta 1}^{\alpha 1}u_3 + M_\beta^{\alpha 1}\tau_{33} + M_\beta^{\alpha 2}D_3 \\ D_\rho = J_\rho^{\alpha 2}\tau_{\alpha 3} - \left(r_0 r^{-1}K_{1\rho}^{22}\partial_1 + K_{2\rho}^{22}\partial_2\right)\varphi \end{gathered} \tag{5}$$

where $\varepsilon = h/a$, a is the circumferential length of the inner surface, and

$$\boldsymbol{F} = [u_1 \quad u_2 \quad \tau_{33} \quad D_3]^T, \qquad \boldsymbol{G} = [\tau_{13} \quad \tau_{23} \quad u_3 \quad \varphi]^T \tag{6}$$

The 4×4 diagonal matrix $\tilde{\boldsymbol{A}}$ is denoted as $\tilde{\boldsymbol{A}} = \text{diag}[0, 0, 1, 0]$. $\boldsymbol{Q}_F$ and $\boldsymbol{Q}_G$, as well as their inverses $\boldsymbol{Q}_F^{-1}$ and $\boldsymbol{Q}_G^{-1}$, are 4×4 diagonal operator matrices defined by

$$\begin{gathered} \boldsymbol{Q}_F = \text{diag}[r\,Qr^{-1},\ Q,\ r^{-1}Qr,\ r^{-1}Qr] \\ \boldsymbol{Q}_G = \text{diag}[r^{-2}Qr^2,\ r^{-1}Qr,\ Q,\ Q] \end{gathered} \tag{7}$$

$$\begin{gathered} \boldsymbol{Q}_F^{-1} = \text{diag}\left[r\partial_z r^{-1},\ \partial_z,\ r^{-1}\partial_z r,\ r^{-1}\partial_z r\right] \\ \boldsymbol{Q}_G^{-1} = \text{diag}\left[r^{-2}\partial_z r^2,\ r^{-1}\partial_z r,\ \partial_z,\ \partial_z\right] \end{gathered} \tag{8}$$

where

$$Q(\cdots) \equiv \int_0^z (\cdots)\,\mathrm{d}z, \qquad \partial_z \equiv \frac{\partial}{\partial z} \tag{9}$$

and we have used the scaled thickness coordinate $z = x_3/\varepsilon$. Thus, z varies from 0 to a as x_3 goes from 0 to h. The 4×4 operator matrices $\boldsymbol{A}$ and $\boldsymbol{B}$ contain the differential operator $\partial_\alpha \equiv \partial/\partial_\alpha$ and depend on z as

Received 11 December 2000; revision received 7 June 2001; accepted for publication 20 July 2001.

*Research Associate, Department of Mechanical Engineering.
†Distinguished Professor and Holder of Oscar S. Wyatt Chair, Department of Mechanical Engineering. Associate Fellow AIAA.

$$\boldsymbol{A}=\begin{bmatrix}\boldsymbol{I} & -r_0r^{-1}\boldsymbol{J}_1\partial_1-\boldsymbol{J}_2\partial_2\\ -r_0r^{-1}\boldsymbol{J}_1^T\partial_1-\boldsymbol{J}_2^T\partial_2 & r_0^2r^{-2}\boldsymbol{K}_{11}\partial_{11}+r_0r^{-1}(\boldsymbol{K}_{12}+\boldsymbol{K}_{21})\partial_{12}+\boldsymbol{K}_{22}\partial_{22}\end{bmatrix}$$

$$\boldsymbol{B}=\begin{bmatrix}-r_0^2r^{-2}\boldsymbol{L}_{11}\partial_{11}-r_0r^{-1}(\boldsymbol{L}_{12}+\boldsymbol{L}_{21})\partial_{12}-\boldsymbol{L}_{22}\partial_{22} & -r_0r^{-1}\boldsymbol{M}_1\partial_1-\boldsymbol{M}_2\partial_2\\ -r_0r^{-1}\boldsymbol{M}_1^T\partial_1-\boldsymbol{M}_2^T\partial_2 & \boldsymbol{N}\end{bmatrix} \tag{10}$$

The nonzero elements of the matrix $\boldsymbol{P}$ are only on the third row:

$$P_{3\omega}=(\varepsilon r)^{-1}\left(r_0r^{-1}L_{11}^{1\omega}\partial_1+L_{12}^{1\omega}\partial_2\right)$$

$$P_{33}=(\varepsilon r)^{-1}M_1^{11},\qquad P_{34}=(\varepsilon r)^{-1}M_1^{12} \tag{11}$$

As defined in previous work,[5–9] the matrices $\boldsymbol{I},\boldsymbol{N},\boldsymbol{J}_\beta,\boldsymbol{M}_\beta,\boldsymbol{K}_{\beta\rho}$, and $\boldsymbol{L}_{\beta\rho}$ are only related to the material properties:

$$\boldsymbol{I}=(I^{\omega\alpha})=\begin{bmatrix}c_{1313} & c_{1323}\\ c_{1323} & c_{2323}\end{bmatrix}^{-1},\qquad \boldsymbol{N}=(N^{\alpha\omega})=\begin{bmatrix}c_{3333} & e_{333}\\ e_{333} & -k_{33}\end{bmatrix}^{-1}$$

$$\begin{bmatrix}J_\beta^{\omega 1} & J_\beta^{\omega 2}\end{bmatrix}=\begin{bmatrix}\delta_{\omega\beta} & I^{\omega\alpha}e_{\beta\alpha 3}\end{bmatrix}$$

$$\begin{bmatrix}M_\beta^{\alpha 1} & M_\beta^{\alpha 2}\end{bmatrix}=[c_{\alpha\beta 33}\quad e_{3\alpha\beta}]\boldsymbol{N}$$

$$K_{\beta\rho}^{11}=K_{\beta\rho}^{12}=K_{\beta\rho}^{21}=0,\qquad K_{\beta\rho}^{22}=J_\beta^{\omega 2}e_{\rho\omega 3}+k_{\beta\rho}$$

$$L_{\beta\rho}^{\alpha\omega}=c_{\alpha\beta\omega\rho}-M_\beta^{\alpha 1}c_{33\omega\rho}-M_\beta^{\alpha 2}e_{3\omega\rho} \tag{12}$$

Other notations include $\eta=(\varepsilon r)^{-2}L_{11}^{11}$ and the Kronecker delta $\delta_{\omega\beta}$.

III. Asymptotic Theory

To establish an asymptotic theory of successive approximations, the functions $\boldsymbol{F}$ and $\boldsymbol{G}$ are expanded in terms of the small thickness parameter ε as

$$\begin{bmatrix}\boldsymbol{F}\\ \boldsymbol{G}\end{bmatrix}=\sum_{n=0}^{\infty}\varepsilon^{2n}\begin{bmatrix}\varepsilon\boldsymbol{f}^{(n)}\\ \boldsymbol{g}^{(n)}\end{bmatrix} \tag{13}$$

Substituting Eq. (13) into Eq. (4) leads to the recurrence relations as

$$\boldsymbol{Q}_G^{-1}\boldsymbol{g}^{(0)}=\boldsymbol{0},\qquad \boldsymbol{Q}_G^{-1}\boldsymbol{g}^{(n+1)}=\boldsymbol{B}\boldsymbol{f}^{(n)}-\boldsymbol{P}^T\boldsymbol{g}^{(n)}$$

$$\boldsymbol{Q}_F^{-1}\boldsymbol{f}^{(0)}=\boldsymbol{A}\,\boldsymbol{g}^{(0)},\qquad \boldsymbol{Q}_F^{-1}\boldsymbol{f}^{(n+1)}=\boldsymbol{A}\,\boldsymbol{g}^{(n+1)}+\boldsymbol{P}\boldsymbol{f}^{(n)}+\eta\tilde{\boldsymbol{A}}\,\boldsymbol{g}^{(n)}$$

$$(n\geq 0) \tag{14}$$

The electromechanical loads on the inner and outer surfaces of the circular cylindrical panel are scaled to be

$$\tau_{\alpha 3}(x_\rho,0)=\varepsilon^2q_\alpha^-(x_\rho),\qquad \tau_{\alpha 3}(x_\rho,a)=\varepsilon^2q_\alpha^+(x_\rho) \tag{15}$$

$$\tau_{33}(x_\rho,0)=-\varepsilon^3q_3^-(x_\rho),\qquad \tau_{33}(x_\rho,a)=-\varepsilon^3q_3^+(x_\rho) \tag{16}$$

$$\varphi(x_\rho,0)=\varepsilon^2V^-(x_\rho),\qquad \varphi(x_\rho,a)=\varepsilon^2V^+(x_\rho) \tag{17}$$

where $q_\alpha^\pm$, $q_3^\pm$, and $V^\pm$ are the tangential tractions, the normal pressures, and the electric potentials applied on the shell surfaces.

Integrating Eqs. (14) with respect to z and considering Eqs. (15–17) for the bottom surface yields

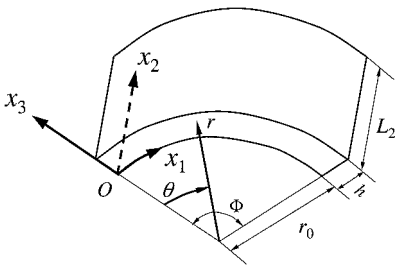

Fig. 1 Geometry of a circular cylindrical shell.

$$\boldsymbol{g}^{(0)}=\begin{bmatrix}0\\ 0\\ U_3^{(0)}\\ 0\end{bmatrix}$$

$$\boldsymbol{g}^{(n+1)}=\begin{bmatrix}r_0^2r^{-2}q_1^-\delta_{n0}\\ r_0r^{-1}q_2^-\delta_{n0}\\ U_3^{(n+1)}\\ V^-\delta_{n0}\end{bmatrix}+\boldsymbol{Q}_G\left(\boldsymbol{B}\boldsymbol{f}^{(n)}-\boldsymbol{P}^T\boldsymbol{g}^{(n)}\right)$$

$$\boldsymbol{f}^{(0)}=\begin{bmatrix}r_0^{-1}rU_1^{(0)}-z\partial_1U_3^{(0)}\\ U_2^{(0)}-z\partial_2U_3^{(0)}\\ 0\\ r_0r^{-1}D_0^{(0)}\end{bmatrix}$$

$$\boldsymbol{f}^{(n+1)}=\begin{bmatrix}r_0^{-1}rU_1^{(n+1)}\\ U_2^{(n+1)}\\ -r_0r^{-1}q_3^-\delta_{n0}\\ r_0r^{-1}D_0^{(n+1)}\end{bmatrix}+\boldsymbol{Q}_F\left(\boldsymbol{A}\,\boldsymbol{g}^{(n+1)}+\boldsymbol{P}\boldsymbol{f}^{(n)}+\eta\tilde{\boldsymbol{A}}\,\boldsymbol{g}^{(n)}\right)$$

$$(n\geq 0) \tag{18}$$

The basic unknowns are the mechanical displacements and the electric displacement at the reference surface $z=0$ of the shell:

$$U_i^{(n)}\equiv u_i^{(n)}(x_\rho,0),\qquad D_0^{(n)}\equiv D_3^{(n)}\left(x_\rho,0^+\right) \tag{19}$$

These unknowns remain to be determined such that the conditions (15–17) for the tractions and the electric potential on the outer surface $z=a$ are satisfied.

According to Eqs. (18), $\boldsymbol{f}^{(n)}$ and $g_3^{(n)}$ can be alternatively written as

$$\boldsymbol{f}^{(n)}=\boldsymbol{X}^{(n)}+\boldsymbol{H}^{(n)},\qquad g_3^{(n)}=U_3^{(n)}+\tilde{H}^{(n)} \tag{20}$$

where

$$\boldsymbol{X}^{(n)}=\begin{bmatrix}r_0^{-1}rU_1^{(n)}-z\partial_1U_3^{(n)}\\ U_2^{(n)}-z\partial_2U_3^{(n)}\\ 0\\ r_0r^{-1}D_0^{(n)}\end{bmatrix},\qquad \boldsymbol{H}^{(0)}=\boldsymbol{0},\qquad \tilde{H}^{(0)}=0$$

$$\boldsymbol{H}^{(n+1)}=\delta_{n0}\left\{\boldsymbol{Q}_F\boldsymbol{A}\begin{bmatrix}r_0^2r^{-2}q_1^-\\ r_0r^{-1}q_2^-\\ 0\\ V^-\end{bmatrix}-\begin{bmatrix}0\\ 0\\ r_0r^{-1}q_3^-\\ 0\end{bmatrix}\right\}$$

$$+\boldsymbol{Q}_F\boldsymbol{A}\boldsymbol{Q}_G\left(\boldsymbol{B}\boldsymbol{f}^{(n)}-\boldsymbol{P}^T\boldsymbol{g}^{(n)}\right)+\boldsymbol{Q}_F\left(\boldsymbol{P}\boldsymbol{f}^{(n)}+\eta\tilde{\boldsymbol{A}}\boldsymbol{g}^{(n)}\right)$$

$$\tilde{H}^{(n+1)}=Q\left(B_{3L}f_L^{(n)}-P_{33}^Tg_3^{(n)}\right)\qquad (n\geq 0) \tag{21}$$

and where an uppercase subscript L takes the values from 1 to 4 and the implicit summation convention applies as usual.

When the integral operator is denoted

$$\bar{Q}(\cdots) \equiv \int_0^a (\cdots)\,\mathrm{d}z \tag{22}$$

the following matrix equation is derived through Eqs. (21) and the traction and electric potential conditions (15–17) for the outer surface:

$$\tilde{\boldsymbol{R}}\tilde{\boldsymbol{X}}^{(n)} = \delta_{n0}\boldsymbol{Y} - \boldsymbol{R}\boldsymbol{H}^{(n)} + \boldsymbol{T}\tilde{H}^{(n)} \tag{23}$$

where

$$\tilde{\boldsymbol{X}}^{(n)} = \left[U_1^{(n)} \quad U_2^{(n)} \quad U_3^{(n)} \quad D_0^{(n)}\right]^T \tag{24}$$

The expressions of the components of the operator matrices $\tilde{\boldsymbol{R}}$, $\boldsymbol{R}$, and $\boldsymbol{T}$ are given in the Appendix. The components of $\boldsymbol{Y}$ on the right-hand side of Eq. (23) contain the electromechanical loads as

$$Y_1 = \left(1 + hr_0^{-1}\right)^2 q_1^+ - q_1^-, \qquad Y_2 = \left(1 + hr_0^{-1}\right) q_2^+ - q_2^-$$

$$Y_3 = -\left(1 + hr_0^{-1}\right) q_3^+ + q_3^- + \left(1 + hr_0^{-1}\right) a\partial_\alpha q_\alpha^+$$

$$Y_4 = V^+ - V^- \tag{25}$$

Equation (23) is the field equation established in the asymptotic theory. The unknowns (24) of each order remain to be solved with specified edge conditions. Because $\boldsymbol{H}^{(0)} = \boldsymbol{0}$, $\tilde{H}^{(0)} = 0$, and $\boldsymbol{Y}$ is known as in Eq. (25) a priori, the leading-order unknowns can be determined from the leading-order field equation. Then $\boldsymbol{H}^{(1)}$ and $\tilde{H}^{(1)}$ can be obtained from Eqs. (20) and (21). Such a procedure may be continued to solve higher-order unknowns. Because the operator matricies $\tilde{\boldsymbol{R}}$, $\boldsymbol{R}$, and $\boldsymbol{T}$ involved in Eq. (23) do not change their forms in the field equations of any order, this makes the solution procedure easier. On the basis of this asymptotic theory, a numerical method may be developed to successively solve the two-dimensional equations with the same operator matrices and then to generate three-dimensional solutions.

IV. Examples

A circular cylindrical panel with central angle Φ and axial length L_2 is considered in the following illustrative examples. The nonzero electromechanical loads are only applied on the outer surface as

$$q_3^+ = \hat{q}_3^+ \sin l_1 x_1 \sin l_2 x_2, \qquad V^+ = -\hat{V}^+ \sin l_1 x_1 \sin l_2 x_2 \tag{26}$$

where

$$l_1 = \pi/a, \qquad l_2 = \pi/L_2, \qquad a = r_0\Phi \tag{27}$$

and a quantity with a superimposed hat denotes the amplitude of the corresponding physical quantity. The mechanical and electrical boundary conditions for simply supported edges

$$u_2 = u_3 = \tau_{11} = \varphi = 0 \qquad \text{at} \qquad x_1 = 0, a$$

$$u_1 = u_3 = \tau_{22} = \varphi = 0 \qquad \text{at} \qquad x_2 = 0, L_2 \tag{28}$$

can be satisfied by assuming

$$\tilde{\boldsymbol{X}}^{(n)} = \begin{bmatrix} U_1^{(n)} \\ U_2^{(n)} \\ U_3^{(n)} \\ D_0^{(n)} \end{bmatrix} = \begin{bmatrix} \hat{U}_1^{(n)} \cos l_1 x_1 \sin l_2 x_2 \\ \hat{U}_2^{(n)} \sin l_1 x_1 \cos l_2 x_2 \\ \hat{U}_3^{(n)} \sin l_1 x_1 \sin l_2 x_2 \\ \hat{D}_0^{(n)} \sin l_1 x_1 \sin l_2 x_2 \end{bmatrix} \tag{29}$$

The physical quantities are nondimensionalized by

$$\bar{u}_i = \hat{u}_i / PL_1, \qquad \bar{\tau}_{ij} = \hat{\tau}_{ij} \big/ Pc^*$$

$$\bar{\varphi} = e^*\hat{\varphi} \big/ PL_1c^*, \qquad \bar{D}_i = \hat{D}_i \big/ Pe^* \tag{30}$$

where either $P = \hat{q}_3^+/c^*$ for applied load q_3^+ or $P = \hat{V}^+(e^*/L_1c^*)$ for applied potential V^+. $L_1 = R\Phi$ and $R = r_0 + h/2$ are the circumferential length and radius of the middle surface.

Three different materials are used to examine the present asymptotic theory. They are polyvinylidene fluoride (PVDF1 and PVDF2) and lead zirconate titanate (PZT-4), and their material moduli are given in Table 1.[20–22]

The present results for an infinitely long single-layer circular cylindrical (PVDF1) piezoelectric panel ($\Phi = \pi/3$) are compared with the available exact solution[20] in Tables 2 and 3, for which $c^* = 2$ GPa and $e^* = 0.06$ C/m^2 have been taken. Selected results for the radius-to-thickness ratio $R/h = 4$ and 10 are given. The leading-order, first-order, and second-order solutions are listed in comparison with the converged higher-order solution that is accurate to four significant digits. The converged orders are shown to be the fifth order and third order for $R/h = 4$ and 10 under the mechanical load, and fifth order and fourth order for $R/h = 4$ and 10 under the electric load. Thus, subsequent higher-order solutions are not necessary. As observed, the converged solutions are in excellent agreement with the exact results. The present asymptotic theory provides fast convergence for the considered example, for which the second-order solution already gives good approximations.

The second example presents the electromechanical analysis of a four-ply (0-deg PVDF2/PZT-4/90-deg PVDF2/PZT-4 starting from the outer ply) laminated circular cylindrical panel ($\Phi = \pi/3$,

Table 1 Material moduli

Moduli	PVDF1	PZT-4	PVDF2
c_{1111}, GPa	3	139	238.24
c_{2222}, GPa	3	139	23.6
c_{3333}, GPa	3	115	10.64
c_{1122}, GPa	1.5	77.8	3.98
c_{1133}, GPa	1.5	74.3	2.19
c_{2233}, GPa	1.5	74.3	1.92
c_{2323}, GPa	0.75	25.6	2.15
c_{3131}, GPa	0.75	25.6	4.4
c_{1212}, GPa	0.75	30.6	6.43
e_{311}, C/m^2	0.0285	−5.2	−0.13
e_{322}, C/m^2	−0.0015	−5.2	−0.145
e_{333}, C/m^2	−0.051	15.1	−0.276
e_{223}, C/m^2	0	12.7	−0.009
e_{113}, C/m^2	0	12.7	−0.135
k_{11}/k_0^a	$106.2/k_0$	1475	12.5
k_{22}/k_0^a	$106.2/k_0$	1475	11.98
k_{33}/k_0^a	$106.2/k_0$	1300	11.98

[a]Here $k_0 = 8.854185$ pF/m.

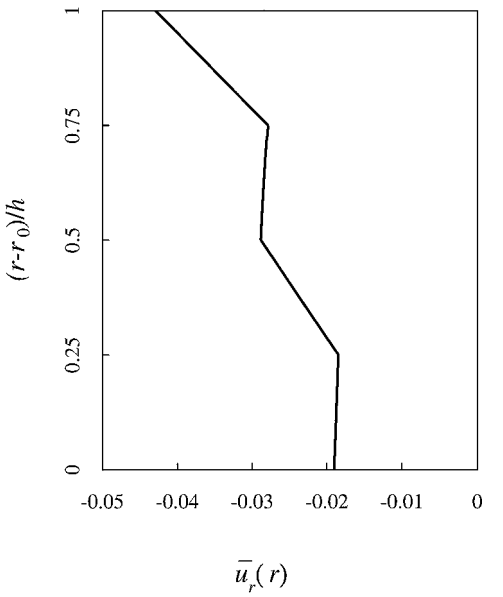

Fig. 2 Through-the-thickness distribution of the deflection for a four-ply laminated circular cylindrical panel under electric load ($\Phi = \pi/3$, $R/h = 20$, and $L_1/L_2 = 1$).

Table 2 Comparison of the present results with exact solution for an infinitely long single-layer piezoelectric circular cylindrical panel under mechanical load ($\Phi = \pi/3$)

Order	$\bar{u}_\theta(0)$	$\bar{u}_r(h/2)$	$\bar{\tau}_{\theta\theta}(0)$	$\bar{\tau}_{r\theta}(h/2)$	$\bar{\varphi}(h/2)$	$\bar{D}_\theta(h/2)$	$\bar{D}_r(0^+)$
			$R/h = 4$				
0	−7.479	−11.22	15.28	0	0	0	0.512
1	−7.990	−12.90	15.58	−2.507	0.010634	−1.971	1.077
2	−8.000	−12.90	15.58	−2.495	0.009260	−1.716	1.017
5	−8.000	−12.90	15.58	−2.495	0.009331	−1.729	1.020
Exact[20]	−8.000	−12.90	15.58	−2.495	0.009331	−1.730	1.020
			$R/h = 10$				
0	−76.94	−164.9	82.77	0	0	0	1.1043
1	−78.03	−168.8	83.03	−5.897	0.02496	−4.626	0.7900
2	−78.08	−168.9	83.04	−5.893	0.02444	−4.531	0.7829
3	−78.08	−168.9	83.04	−5.893	0.02445	−4.531	0.7830
Exact[20]	−78.08	−168.8	83.04	−5.893	0.02445	−4.531	0.7830

Table 3 Comparison of the present results with exact solution for an infinitely long single-layer piezoelectric circular cylindrical panel under electric load ($\Phi = \pi/3$)

Order	$\bar{u}_\theta(0)$	$\bar{u}_r(h/2)$	$\bar{\tau}_{\theta\theta}(h)$	$\bar{\tau}_{r\theta}(h/4)$	$\bar{\varphi}(h/2)$	$\bar{D}_\theta(h)$	$\bar{D}_r(0^+)$
			$R/h = 4$				
0	−1.1937	−0.3979	0	0	0	0	286.7
1	−0.5274	0.4973	−0.3043	0.00000	−0.5313	164.8	260.1
2	−0.5519	0.4752	−0.3341	0.02504	−0.4959	164.8	261.8
5	−0.5511	0.4758	−0.3315	0.02569	−0.4978	164.8	261.7
Exact[20]	−0.5512	0.4760	−0.3314	0.02569	−0.4978	164.8	261.7
			$R/h = 10$				
0	−2.997	−0.9992	0	0	0	0	663.1
1	−2.207	0.6386	−0.1360	0.000000	−0.5125	176.5	653.3
2	−2.210	0.6340	−0.1409	0.004087	−0.5069	176.5	653.4
4	−2.210	0.6340	−0.1408	0.004172	−0.5070	176.5	653.4
Exact[20]	−2.210	0.6340	−0.1408	0.004172	−0.5070	176.6	653.3

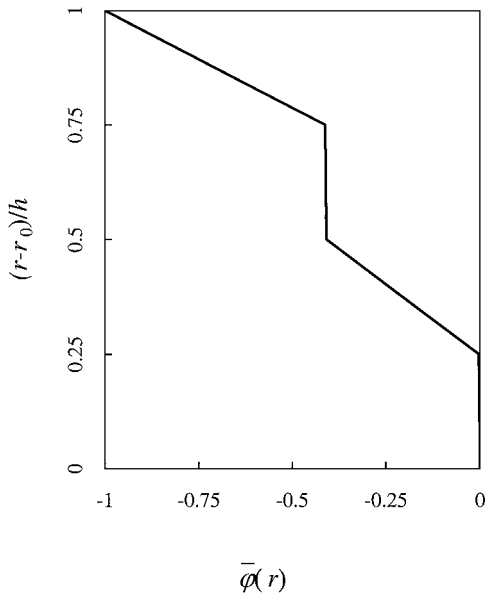

Fig. 3 Through-the-thickness distribution of the electric potential for a four-ply laminated circular cylindrical panel under electric load ($\Phi = \pi/3$, $R/h = 20$, and $L_1/L_2 = 1$).

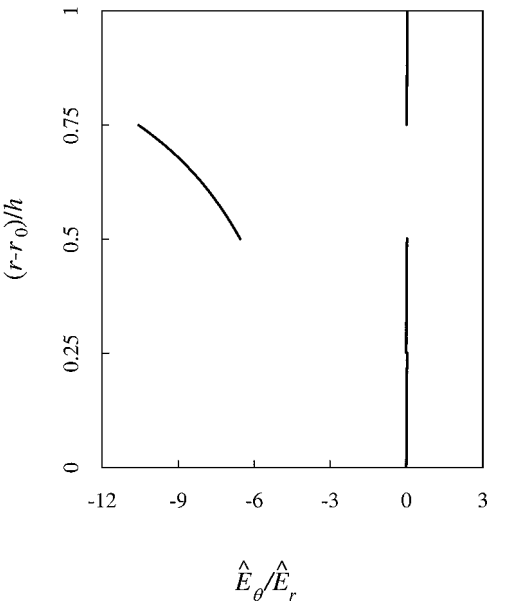

Fig. 4 Through-the-thickness distribution of the amplitude ratio of the circumferential to transverse electric field components for a four-ply laminated circular cylindrical panel under electric load ($\Phi = \pi/3$, $R/h = 20$, and $L_1/L_2 = 1$).

$R/h = 20$, and $L_1/L_2 = 1$). The panel has equal ply thickness and finite axial length. The dimensionless values are also defined by Eq. (30), where $c^* = 1$ GPa and $e^* = 1$ C/m^2.

Figure 2 shows the through-thickness distribution of the deflection of the circular cylindrical panel under the electric voltage. The distribution is approximately piecewise linear through the entire plate thickness. More specifically, the deflection is approximately constant through the thickness of each PZT-4 layer, whereas it is approximately linearly distributed through the thickness of each PVDF2 layer.

The through-thickness electric potential for the laminated circular cylindrical panel under the electric load is presented in Fig. 3. It is appropriate to make an assumption of a piecewise linear distribution of the electric potential through the thickness of a circular cylindrical shell in the case of an applied electric voltage.

As revealed earlier in the plate analyses,[1,5–8] the assumption of negligible in-plane electric field components is not valid in some cases. That is because the in-plane electric field components, when compared with the transverse electric field, are of the order of the reciprocal of the plate thickness parameter. The numerical result given in Fig. 4 for the through-thickness distribution of $\hat{E}_\theta/\hat{E}_r$ clearly demonstrates that such a conclusion also applies to the circular

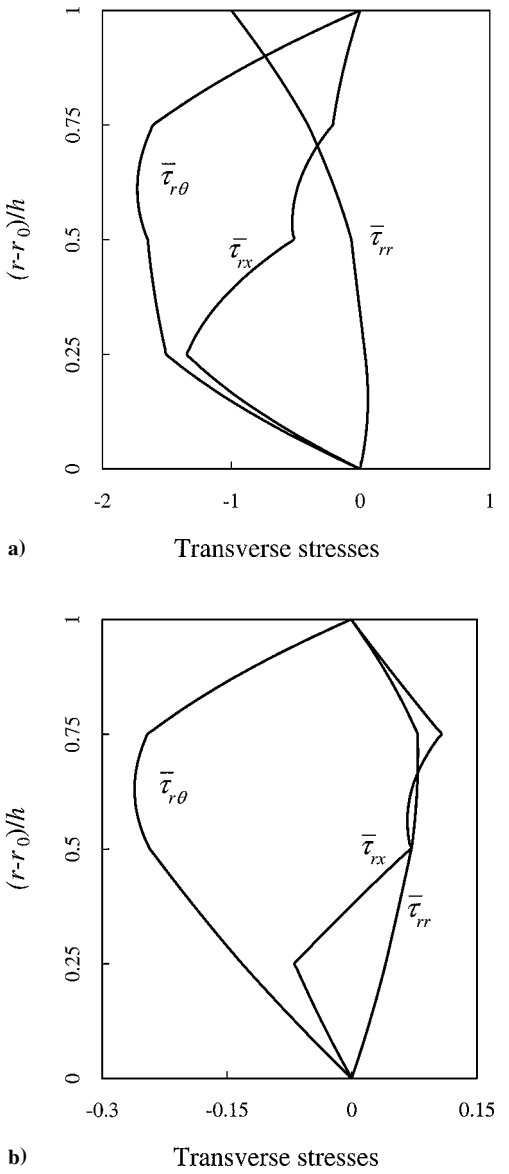

Fig. 5 Through-the-thickness distribution of the deflection for a four-ply laminated circular cylindrical panel under a) mechanical load and b) electric load ($\Phi = \pi/3$, $R/h = 20$, and $L_1/L_2 = 1$).

cylindrical panel. Although the in-plane electric field component is negligibly small in three layers, it is more significant than the transverse electric field component in one PZT-4 layer. The discontinuity of the curve through the thickness is due to the discontinuity of the transverse electric field component.

The through-thickness distributions of the transverse shear and normal stresses are given in Figs. 5a and 5b for the cases of applied mechanical load and applied electric load, respectively. The linear superposition principle applies to the problem so that results due to combined loads may be obtained through respective solution due to simple loading. Therefore, according to Figs. 5a and 5b, the interfacial shear stresses $\tau_{r\theta}$ and τ_{rx} can be reduced in a controlled manner by properly applied electromechanical loads to prevent possible premature shearing delamination.

V. Conclusions

An asymptotic theory has been presented for laminated circular cylindrical piezoelectric shells in the framework of three-dimensional electroelasticity. Solutions can be obtained using a recurrence procedure to desired accuracy for the interiors of the shells. The present results show excellent agreement with the available exact solution. The graphical results provide guidance for making appropriate assumptions in developing new theories.

Appendix: Expressions of the Operator Components

$$\tilde{R}_{11} = -r_0^{-1}\bar{Q}rL_{11}^{11}\partial_{11} - 2r_0^{-2}\bar{Q}r^2L_{12}^{11}\partial_{12} - r_0^{-3}\bar{Q}r^3L_{22}^{11}\partial_{22}$$

$$\tilde{R}_{12} = -\bar{Q}L_{11}^{12}\partial_{11} - r_0^{-1}\bar{Q}r\left(L_{12}^{12} + L_{22}^{11}\right)\partial_{12} - r_0^{-2}\bar{Q}r^2L_{22}^{12}\partial_{22}$$

$$\tilde{R}_{13} = \bar{Q}zL_{11}^{11}\partial_{111} + \bar{Q}z\left(1 + 2r_0^{-1}r\right)L_{12}^{11}\partial_{112} + r_0^{-1}\bar{Q}zr\left[L_{12}^{12} + \left(1 + r_0^{-1}r\right)L_{22}^{11}\right]\partial_{122} + r_0^{-2}\bar{Q}zr^2L_{22}^{12}\partial_{222} - T_1$$

$$\tilde{R}_{14} = -\bar{Q}M_1^{12}\partial_1 - r_0^{-1}\bar{Q}rM_2^{12}\partial_2$$

$$\tilde{R}_{22} = -r_0\bar{Q}r^{-1}L_{22}^{11}\partial_{11} - 2\bar{Q}L_{22}^{12}\partial_{12} - r_0^{-1}\bar{Q}rL_{22}^{22}\partial_{22}$$

$$\tilde{R}_{23} = r_0\bar{Q}zr^{-1}L_{12}^{11}\partial_{111} + \bar{Q}z\left[\left(1 + r_0r^{-1}\right)L_{22}^{11} + L_{12}^{12}\right]\partial_{112} + \bar{Q}z\left(2 + r_0^{-1}r\right)L_{22}^{12}\partial_{122} + r_0^{-1}\bar{Q}zrL_{22}^{22}\partial_{222} - T_2$$

$$\tilde{R}_{24} = -r_0\bar{Q}r^{-1}M_1^{22}\partial_1 - \bar{Q}M_2^{22}\partial_2$$

$$\tilde{R}_{33} = r_0\bar{Q}z^2r^{-1}L_{11}^{11}\partial_{1111} + 2\bar{Q}z^2\left(1 + r_0r^{-1}\right)L_{12}^{11}\partial_{1112} + \bar{Q}z^2\left[2L_{12}^{12} + \left(2 + r_0r^{-1} + r_0^{-1}r\right)L_{22}^{11}\right]\partial_{1122} + 2\bar{Q}z^2\left(1 + r_0^{-1}r\right)L_{22}^{12}\partial_{1222} + r_0^{-1}\bar{Q}z^2rL_{22}^{22}\partial_{2222} - 2T_3 - \varepsilon^{-2}r_0^{-1}\bar{Q}r^{-1}L_{11}^{11}$$

$$\tilde{R}_{34} = -r_0\bar{Q}zr^{-1}M_1^{12}\partial_{11} - \bar{Q}z\left(1 + r_0r^{-1}\right)M_2^{12}\partial_{12} - \bar{Q}zM_2^{22}\partial_{22} + T_4$$

$$\tilde{R}_{44} = r_0\bar{Q}r^{-1}N^{22}$$

$$\tilde{R}_{21} = \tilde{R}_{12}, \qquad \tilde{R}_{3\alpha} = -\tilde{R}_{\alpha 3}, \qquad \tilde{R}_{4\alpha} = \tilde{R}_{\alpha 4}, \qquad \tilde{R}_{43} = -\tilde{R}_{34}$$

$$R_{11} = -\bar{Q}L_{11}^{11}\partial_{11} - 2r_0^{-1}\bar{Q}rL_{12}^{11}\partial_{12} - r_0^{-2}\bar{Q}r^2L_{22}^{11}\partial_{22}$$

$$R_{12} = \tilde{R}_{12}$$

$$R_{13} = -r_0^{-1}\bar{Q}rM_1^{11}\partial_1 - r_0^{-2}\bar{Q}r^2M_2^{11}\partial_2$$

$$R_{14} = -r_0^{-1}\bar{Q}rM_1^{12}\partial_1 - r_0^{-2}\bar{Q}r^2M_2^{12}\partial_2$$

$$R_{21} = -r_0\bar{Q}r^{-1}L_{11}^{12}\partial_{11} - \bar{Q}\left(L_{12}^{12} + L_{22}^{11}\right)\partial_{12} - r_0^{-1}\bar{Q}rL_{22}^{12}\partial_{22}$$

$$R_{22} = \tilde{R}_{22}$$

$$R_{23} = -\bar{Q}M_1^{21}\partial_1 - r_0^{-1}\bar{Q}rM_2^{21}\partial_2$$

$$R_{24} = -\bar{Q}M_1^{22}\partial_1 - r_0^{-1}\bar{Q}rM_2^{22}\partial_2$$

$$R_{31} = -r_0\bar{Q}zr^{-1}L_{11}^{11}\partial_{111} - \bar{Q}z\left(2 + r_0r^{-1}\right)L_{12}^{11}\partial_{112} - \bar{Q}z\left[L_{12}^{12} + \left(1 + r_0^{-1}r\right)L_{22}^{11}\right]\partial_{122} - r_0^{-1}\bar{Q}zrL_{22}^{12}\partial_{222} + \varepsilon^{-1}\bar{Q}r^{-1}L_{11}^{11}\partial_1 + \varepsilon^{-1}r_0^{-1}\bar{Q}L_{12}^{11}\partial_2$$

$$R_{32} = \tilde{R}_{32}$$

$$R_{33} = -\bar{Q}zM_1^{11}\partial_{11} - \bar{Q}z\left(1 + r_0^{-1}r\right)M_2^{11}\partial_{12} - r_0^{-1}\bar{Q}zrM_2^{21}\partial_{22} + \varepsilon^{-1}r_0^{-1}\bar{Q}M_1^{11}$$

$$R_{34} = -\bar{Q}zM_1^{12}\partial_{11} - \bar{Q}z\left(1 + r_0^{-1}r\right)M_2^{12}\partial_{12} - r_0^{-1}\bar{Q}zrM_2^{22}\partial_{22} + \varepsilon^{-1}r_0^{-1}\bar{Q}M_1^{12}$$

$$R_{41} = -r_0\bar{Q}r^{-1}M_1^{12}\partial_1 - \bar{Q}M_2^{12}\partial_2$$

$$R_{42} = \tilde{R}_{42}$$

$$R_{43} = \bar{Q}N^{21}$$

$$R_{44} = \bar{Q}N^{22}$$

$$T_1 = \varepsilon^{-1}r_0^{-1}\bar{Q}L_{11}^{11}\partial_1 + \varepsilon^{-1}r_0^{-2}\bar{Q}rL_{12}^{11}\partial_2$$

$$T_2 = \varepsilon^{-1}\bar{Q}r^{-1}L_{11}^{12}\partial_1 + \varepsilon^{-1}r_0^{-1}\bar{Q}L_{12}^{12}\partial_2$$

$$T_3 = \varepsilon^{-1}\bar{Q}zr^{-1}L_{11}^{11}\partial_{11} + \varepsilon^{-1}r_0^{-1}\bar{Q}z\left(1 + r_0r^{-1}\right)L_{12}^{11}\partial_{12} + \varepsilon^{-1}r_0^{-1}\bar{Q}zL_{12}^{12}\partial_{22} - \varepsilon^{-2}r_0^{-1}\bar{Q}r^{-1}L_{11}^{11}$$

$$T_4 = \varepsilon^{-1}\bar{Q}r^{-1}M_1^{12}$$

Acknowledgments

The support of this research by the Army Research Office through Grant DAAH 04-96-1-0080 and the Oscar S. Wyatt Chair is gratefully acknowledged.

References

[1]Bisegna, P., and Maceri, F., "An Exact Three-Dimensional Solution for Simply Supported Rectangular Piezoelectric Plates," *Journal of Applied Mechanics*, Vol. 63, No. 3, 1996, pp. 628–638.

[2]Heyliger, P., and Brooks, S., "Exact Solutions for Laminated Piezoelectric Plates in Cylindrical Bending," *Journal of Applied Mechanics*, Vol. 63, No. 4, 1996, pp. 903–910.

[3]Heyliger, P., "Exact Solutions for Simply Supported Laminated Piezoelectric Plates," *Journal of Applied Mechanics*, Vol. 64, No. 2, 1997, pp. 299–306.

[4]Rahmoune, M., Benjeddou, A., Ohayon, R., and Osmont, D., "New Thin Piezoelectric Plate Models," *Journal of Intelligent Material Systems and Structures*, Vol. 9, No. 12, 1998, pp. 1017–1029.

[5]Cheng, Z. Q., Lim, C. W., and Kitipornchai, S., "Three-Dimensional Exact Solution for Inhomogeneous and Laminated Piezoelectric Plates," *International Journal of Engineering Science*, Vol. 37, No. 11, 1999, pp. 1425–1439.

[6]Cheng, Z. Q., Lim, C. W., and Kitipornchai, S., "Three-Dimensional Asymptotic Approach to Inhomogeneous and Laminated Piezoelectric Plates," *International Journal of Solids and Structures*, Vol. 37, No. 15, 2000, pp. 3153–3175.

[7]Cheng, Z.-Q., and Batra, R. C., "Three-Dimensional Asymptotic Analysis of Multiple-Electroded Piezoelectric Laminates," *AIAA Journal*, Vol. 38, No. 2, 2000, pp. 317–324.

[8]Cheng, Z.-Q., and Batra, R. C., "Generalized Plane Solution for Monoclinic Piezoelectric Laminates," *AIAA Journal*, Vol. 38, No. 2, 2000, pp. 335–341.

[9]Cheng, Z. Q., and Batra, R. C., "Three-Dimensional Asymptotic Scheme for Piezothermoelastic Laminates," *Journal of Thermal Stresses*, Vol. 23, No. 2, 2000, pp. 95–110.

[10]Rogers, T. G., Watson, P., and Spencer, A. J. M., "An Exact Three-Dimensional Solution for Normal Loading of Inhomogeneous and Laminated Anisotropic Elastic Plates of Moderate Thickness," *Proceedings of the Royal Society of London*, Vol. A437, No. 1899, 1992, pp. 199–213.

[11]Rogers, T. G., Watson, P., and Spencer, A. J. M., "Exact Three-Dimensional Elasticity Solutions for Bending of Moderately Thick Inhomogeneous and Laminated Strips Under Normal Pressure," *International Journal of Solids and Structures*, Vol. 32, No. 12, 1995, pp. 1659–1673.

[12]Wang, Y. M., and Tarn, J. Q., "A Three-Dimensional Analysis of Anisotropic Inhomogeneous and Laminated Plates," *International Journal of Solids and Structures*, Vol. 31, No. 4, 1994, pp. 497–515.

[13]Tarn, J. Q., and Wang, Y. M., "Asymptotic Thermoelastic Analysis of Anisotropic Inhomogeneous and Laminated Plates," *Journal of Thermal Stresses*, Vol. 18, No. 1, 1995, pp. 35–58.

[14]Tarn, J. Q., "Elastic Buckling of Multilayered Anisotropic Plates," *Journal of the Mechanics and Physics of Solids*, Vol. 44, No. 3, 1996, pp. 389–411.

[15]Tarn, J. Q., "An Asymptotic Theory for Nonlinear Analysis of Multilayered Anisotropic Plates," *Journal of the Mechanics and Physics of Solids*, Vol. 45, No. 7, 1997, pp. 1105–1120.

[16]Maugin, G. A., and Attou, D., "An Asymptotic Theory of Thin Piezoelectric Plates," *Quarterly Journal of Mechanics and Applied Mathematics*, Vol. 43, No. 3, 1990, pp. 347–362.

[17]Bisegna, P., and Maceri, F., "A Consistent Theory of Thin Piezoelectric Plates," *Journal of Intelligent Material Systems and Structures*, Vol. 7, No. 4, 1996, pp. 372–389.

[18]Tarn, J. Q., and Yen, C. B., "A Three-Dimensional Asymptotic Analysis of Anisotropic Inhomogeneous and Laminated Cylindrical Shells," *Acta Mechanica*, Vol. 113, Nos.1–4, 1995, pp. 137–153.

[19]Tiersten, H. F., *Linear Piezoelectric Plate Vibrations*, Plenum, New York, 1969.

[20]Dumir, P. C., Dube, G. P., and Kapuria, S., "Exact Piezoelastic Solution of Simply-Supported Orthotropic Circular Cylindrical Panel in Cylindrical Bending," *International Journal of Solids and Structures*, Vol. 34, No. 6, 1997, pp. 685–702.

[21]Berlincourt, D. A., Curran, D. R., and Jaffe, H., "Piezoelectric and Piezomagnetic Materials and Their Function in Transducers," *Physical Acoustics*, edited by W. P. Mason, Vol. 1, Academic Press, New York, 1964, pp. 169–270.

[22]Tashiro, K., Tadokoro, H., and Kobayashi, M., "Structure and Piezoelectricity of Poly (Vinylidene Fluoride)," *Ferroelectrics*, Vol. 32, Nos.1–4, 1981, pp. 167–175.

A. M. Baz
Associate Editor